Linear optical properties and multiphoton absorption of alkali halides calculated from first principles

Jun Li, Chun-gang Duan, Zong-quan Gu, and Ding-sheng Wang
Laboratory for Surface Physics, Institute of Physics, and Center for Condensed Matter Physics, Academia Sinica, Beijing 100080, China
(Received 13 August 1997)

This paper reports the calculation of linear optical properties and multiphoton absorption (MPA) coefficients of alkali halides $MX(M=\mathrm{Na, K};X=\mathrm{F, Cl,Br, I})$ using the first-principles linearized augmented-plane-wave band method and the time-dependent perturbation theory. The calculations are in good agreement with available experimental data. For linear optical properties, the trend of the static dielectric constants with respect to the halides is attributed to the variation of the optical oscillator strength arising from the electronic transitions of the valence p bands. For MPA coefficients the spectra of two-photon absorption given in the region of photon energy $(\frac{1}{2}E_g, E_g)$ show an increase of MPA coefficients with respect to the atomic number of the halogen elements. The polarization dependence of the MPA coefficients is also given, which promotes further experiments. [S0163-1829(98)08403-3]

I. INTRODUCTION

The multiphoton absorption (MPA) process in crystalline solids, as a nonlinear optical phenomenon, has been investigated extensively using many experimental and theoretical methods since the advent of the laser. Nathan, Guenther, and Mitra[1] made an extensive review of those theoretical works and compared results with available experimental data. In the theoretical part, a time-dependent perturbation approach and simplified empirical band schemes were usually employed. Because of the large discrepancy between the experimental data and the calculation, it was concluded that more reliable calculations should be based on accurate band structures.

It is not trivial to calculate the MPA coefficients from first-principles band calculations because the present tractable first-principles band calculation employing the local-density approximation[2] (LDA) is valid only for the ground state of an inhomogeneous electron system and is not a concept suitable for the excitation problem. However, in practice, the LDA has been accepted as a computationally expeditious way to approach the nonlinear optical problem in recent years.[3–5] Strictly speaking, the validity of the first-principles band theory has not been widely verified for both linear and nonlinear optical properties of ionic crystals, which have received less attention than semiconductors. As many ionic crystals are identified as important materials in laser technology[6,7] and MPA processes are important in laser-induced intrinsic damage,[8] a clear picture is required from the first-principles band theory concerning the optical excitation as well as the nature of the optical properties for ionic crystals.

This paper adopts alkali halides $MX(M=\mathrm{Na, K};X=\mathrm{F, Cl, Br, I})$ as the prototype, as they were used in the experimental studies of MPA. We confine ourselves to the context of the LDA theory to treat the linear response and the nonlinear excitation on an equal footing. In the linear aspect, we pay attention to the nature of the systematic trend in the linear optical properties of MX and the justification of the first-principles calculation. In terms of MPA, attention is paid to the estimation of the MPA coefficients as well as the polarization dependence of the two-photon absorption spectra. In both cases, our attention is focused on the systematic trend of optical properties of MX.

In Sec. II we elucidate the characteristic of the band structure of MX obtained from the linearized augmented-plane-wave (LAPW) method. After outlining the theory of the interband transition in Sec. III, we analyze the mechanism for the trend in the static dielectric constants and justify the present calculation of the linear optical properties by comparing calculated and measured spectra of NaCl and KCl. The time-dependent perturbation theory for the MPA coefficient is outlined in Sec. IV, followed by comparison between its calculated and measured values and a summary of the characters of the MPA coefficients. Section V is a brief conclusion.

II. BAND STRUCTURE

In this paper the self-consistent LAPW method[9,10] with the von Barth–Hedin exchange-correlation term is employed to carry out the band-structure calculation. The lattice parameters[11] used in the calculation are listed in Table I. About 50 LAPW bases per atom are used in solving the semirelativistic Schrödinger equation and 20 special k points in the irreducible Brillouin zone are used in generating the charge density in the self-consistent calculation. The convergence measured by the rms difference between the input and output charge densities is better than 0.01 me/a.u.^{3}

The band structure of alkali halides has been reported extensively.[12] For discussion in later sections, we plot our results in Fig. 1 and summarize the characteristics of their band structures: (i) All the alkali halides considered have direct band gaps at the Γ point. In contrast, in the calculation of Ching, Gan, and Huang,[4] the NaI and KI are reported as an indirect gap. (ii) Three upper valence bands (VB's) consist of the halogen p orbitals (p VB's), while the lower VB

TABLE I. Calculated energy gap (E_g), static dielectric constant (ε_0), and N_{eff} of MX.

Alkali halide	Lattice constant (Å) [a]	Experiment E_g (eV) [b]	Experiment ε_0 [c]	Present E_g (eV)	Present ε_0	Present N_{eff}	Scissors ε_0
NaF	4.63	11.5	1.74	7.26	1.670	3.906	1.317
NaCl	5.64	8.75	2.33	6.38	2.529	6.053	1.819
NaBr	5.97	7.1	2.60	5.84	2.762	6.874	2.194
NaI	6.48	5.9	2.98	4.37	3.394	7.687	2.353
KF	5.35	10.8	1.84	6.23	1.588	4.091	1.230
KCl	6.29	8.7	2.17	5.17	2.268	6.295	1.493
KBr	6.60	7.4	2.35	4.85	2.680	7.363	1.779
KI	7.07	6.34	2.63	4.26	2.842	7.736	1.867

[a]From Ref. 11.
[b]From Ref. 13.
[c]From Ref. 18.

is the halogen s orbital (s VB's). However, the bottom of the conduction band (CB) is a mixture of the alkali metal and halogen s orbitals. (iii) From MF, through MCl and MBr, to MI, the band gap reduces in accordance with the trend observed in the experiments[13] and the width of the p VB increases while the gap between the p VB and s VB reduces. (iv) NaX has a wider VB width and larger gap than the corresponding KX and the gap between the p VB and s VB of NaX is slightly larger than that of KX. Because of the known failure of the LDA on the estimation of the band energy, the calculated gap is lower than the measured one, as usual.

III. LINEAR OPTICAL PROPERTIES

A. Methodology

Within the one-electron picture, the interband optical conductivity tensor is well known as (all formulas in this paper use atomic units)

$$\sigma(\omega)=\frac{2\pi}{\omega\Omega}\sum_{\vec{k}} W_{\vec{k}}\sum_{c,v}|\langle c|\vec{e}\cdot\vec{p}|v\rangle|^2\delta(E_c-E_v-\omega), \quad (1)$$

where Ω is the cell volume, ω the photon energy, $\vec{e}$ the polarization direction of the photon, and $\vec{p}$ the electron momentum operator. The integral over the k space has been replaced by a summation over special k points with corresponding weighting factors $W_{\vec{k}}$. The second summation includes the VB states (v) and CB states (c) and the subscript E is the band energy. In Eq. (1) it is also reasonably assumed that in these wide-gap crystals the VB is fully occupied while the CB is empty. The δ function has been approximated by a Gaussian function in the practical calculation that

$$\delta(x)\approx\frac{1}{\sqrt{\pi}\Gamma}e^{-(x/\Gamma)^2}, \quad (2)$$

where Γ is the Gaussian factor set equal to 0.35 eV for reasons given below.

The imaginary part of the complex dielectric function $\varepsilon_2(\omega)$ is related to $\sigma(\omega)$ by $\varepsilon_2(\omega)=(2\pi/\omega)\sigma(\omega)$ and the real part of the dielectric function $\varepsilon_1(\omega)$ is obtained from the Kramers-Kronig relation

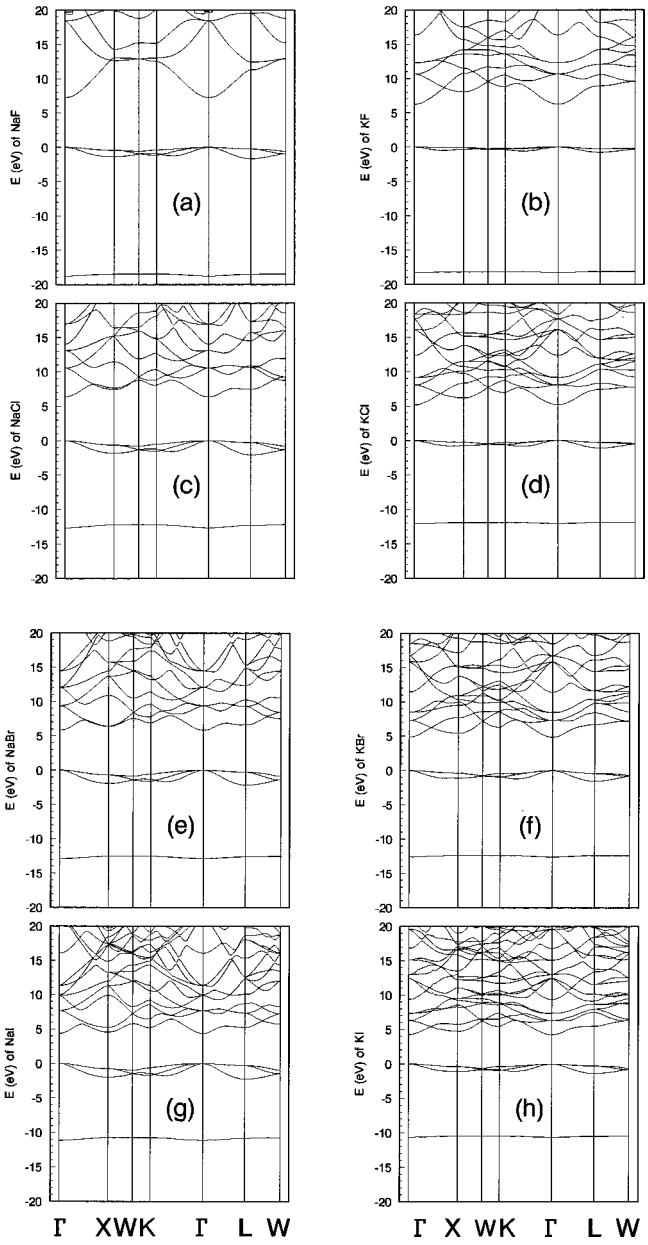

FIG. 1. Band structure of MX (M=Na,K;X=F, Cl, Br, I). Bands are connected by the order in energy.

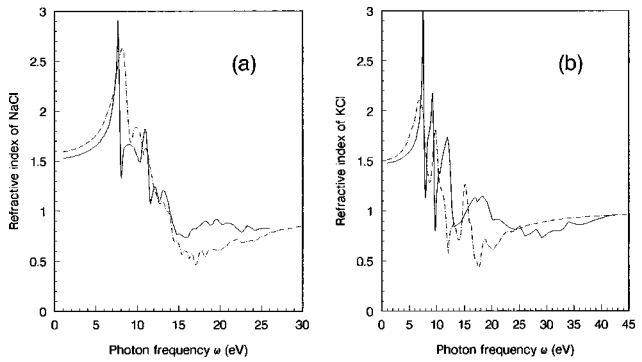

FIG. 2. Calculated refractive index (dashed lines) of NaCl and KCl versus experimental data (solid lines) from Ref. 14.

$$\varepsilon_1(\omega)=1+8\mathrm{P}\int_0^\infty \sigma(\xi)/(\xi^2-\omega^2)d\xi. \tag{3}$$

Here P denotes the principal value integral. The electronic part of the static dielectric constant is thus given by $\varepsilon_0=\varepsilon_1(0)$. Other frequency-dependent linear optical constants can be obtained from the complex dielectric function. In particular, the linear refractive index reads

$$n(\omega)=\left(\frac{\sqrt{\varepsilon_1^2(\omega)+\varepsilon_2^2(\omega)}+\varepsilon_1(\omega)}{2}\right)^{1/2}.$$

In principle, we should integrate formula (3) to infinity for the real part of the dielectric function. In practice, we have to truncate at a higher enough cutoff energy. At present, we are mainly concerned with the valence transition, shown in the measurement of KCl,[14] which dominates the region between the fundamental transition and about 43 eV above. In the higher-energy region, it contains substantially the core excitations. Thus we truncate the photon energy at 45 eV in comparing the integrated optical properties of MX.

An important integrated optical property is the optical oscillator strength, which is defined as the integral of the optical oscillator strength density $(2/\pi)\sigma(\omega)$ with respect to the photon energy:

$$\int_0^{\omega_c}\frac{2}{\pi}\sigma(\omega)d\omega=\frac{N_{eff}}{\Omega}. \tag{4}$$

Here N_{eff} is the effective number of electrons in the unit cell Ω that contribute to the optical oscillator below the truncation energy ω_c. In fact, this formula is the f sum rule for finite energy.[15] As an extension of the proof of this f sum rule for atomic spectra[16] it is easy to show that if we allow the summation over the CB states in Eq. (1) to include the core states and VB states, i.e., covering the whole space spanned by all eigenstates of the Kohn-Sham equation, the corresponding N_{eff} calculated in formula (4) is strictly the occupation number of the initial states.[17] Note that the transitions from the VB states to core states give a negative component in the extended summation, reflecting the exchange of oscillator strength between core states and VB states.[15] Because the transitions from VB states to other occupied states are forbidden by the Pauli principle, the exchange of oscillator strength between core states and VB states made N_{eff} larger than the occupation number of involved VB's if the considered CB's approach the completeness and the truncation energy is high enough in the calculation. This criterion can be employed to judge the convergence of the calculation and analyze the contribution to the optical oscillator.

B. Numerical results and discussion

The momentum matrix elements of MX are calculated at the 44 special k points in the irreducible Brillouin zone. We first consider the three p VB states as initial states. The effect of including the s VB state will be discussed later. The calculated static dielectric constants (Table I) show a trend with respect to the change of either the alkali metal or the halogen elements in agreement with the measurement,[18] with the only exception being the order between NaF and KF when the difference between their experimental data is the smallest and might be less than the error bar of the present calculation. This agreement is better than the previous calculation of Ching, Gan, and Huang.[4]

Because, according to Eq. (3), the static dielectric constant is determined mainly by the contribution of the optical conductivity in the low-photon-energy region, the transitions with p VB's as initial states govern the trend of the static dielectric constants of MX. Their difference is reflected in the effective number of electrons N_{eff} (Table I). Note, as shown in Eqs. (3) and (4), that the difference between ε_0 and N_{eff} is that ε_0 has an energy denominator, while N_{eff} does not. As typical ionic crystals, the VB's of MX are determined by the anion X. The number of core states of the anion increases from MF to MI. Thus, as mentioned in Sec. III A, the exchange of oscillator strength between core states and p VB states increases from MF to MI. This makes N_{eff} of the p VB's increase from MF to MI. For MF, $N_{eff}<6$ indicates that a substantial contribution to the oscillator strength is beyond the present truncation photon energy. An increase in the value of N_{eff} indeed exists for MF by increasing ω_c in the calculation.

The relative error between the calculated and measured static dielectric constants is all below 15%. However, the integrated properties are not enough to judge the validity of the present LDA calculation. We employ the linear refractive index of NaCl and KCl for a detailed comparison (Fig. 2). Indeed, the calculations describe qualitatively the measured spectra with regard to the magnitude, number, and position of the peaks in the refractive index spectra below a photon energy about 10–15 eV. For higher photon energy, the calculations do not reproduce the measured spectra well. The defect of the one-electron picture of the LDA, which generally affects the gap transition more seriously,[19] may lead to deviation most prominently in the region of lower photon energy. The betrayal of the calculation in the higher-energy region, on the other hand, most probably can be attributed to two other causes. First, the transition, for example, from the core states of the sodium and potassium ion contributes to the measured spectra,[14] which is not considered in the present calculation. The second cause is the shortcoming of the present band calculation on the high-lying CB states. As pointed out by Koelling and Arbman,[20] the linearizing technique in the LAPW method allows the energy parameter to

TABLE II. Dependence of two-, three-, and four-photon MPA coefficients $\alpha^{(m)}$ in units of cm^{2m-3}/GW^{m-1} of NaCl on the parameter Γ (eV). Polarization is along [111] and the truncation energy is 60 eV.

Γ (eV)	$\alpha^{(2)}$ (0.266 μm)	$\alpha^{(3)}$ (0.397 μm)	$\alpha^{(4)}$ (0.532 μm)
0.10	2.70	1.67×10^{-5}	4.23×10^{-10}
0.20	3.21	1.57×10^{-5}	4.64×10^{-10}
0.25	3.33	1.61×10^{-5}	6.74×10^{-10}
0.30	3.39	1.65×10^{-5}	1.44×10^{-9}
0.35	3.42	1.70×10^{-5}	2.86×10^{-9}
0.40	3.42	1.73×10^{-5}	4.63×10^{-9}
0.45	3.41	1.76×10^{-5}	6.40×10^{-9}
0.50	3.38	1.79×10^{-5}	7.96×10^{-9}

deviate only within 1 Ry for s and p states for an acceptable calculation. In the present band calculation, the s and p components of the CB states are calculated by the same energy parameter as in the occupied VB states. Thus the present results of CB's of MX are only acceptable in the low-lying CB's, roughly corresponding to the interband transition below a photon energy about 1 Ry.

Now let us consider the contribution from the s VB. In view of energy (Fig. 1), it is possible for the s VB transition to occur as the photon energy reaches about 15 eV for MI, 20 eV for MCl and MBr, and 25 eV for MF, but the transition from the s VB to the low-lying CB's are almost forbidden by the selection rule. When the s VB is included as an initial state, the changes of ε_0 and N_{eff} are less than 0.1% and 1%, respectively.[17] The s VB, according to the present calculation, gives only a negligible contribution. However, this might be incorrect because we did not treat the s VB transition properly for the deficit in the high-lying CB's at present.

In the past, there was a simple correction, the so-called scissors approximation as adopted by Wang and Klein,[21] i.e., a rigid shift was applied on the self-consistent LDA energies of the conduction band to fit the experimentally observed optical gap to investigate the linear optical properties of semiconductors. We also judge the validity of the scissors approximation by presenting its results in the last column of Table I. The scissors approximation obviously leads to worse results and is invalid for the optical processes of ionic crystals such as MX. A similar conclusion has also been derived in the work of Ching and his colleagues.[3,4] The invalidity indicates that the correction of the LDA is dependent on the state of electrons and cannot be described by a rigid shift as shown by Hybertsen and Louie.[22]

IV. MPA COEFFICIENTS

A. Methodology

To calculate the MPA coefficients, we use the conventional time-dependent perturbation theory. The electronic transition probability rate per unit volume between the initial VB states and final CB states by simultaneously absorbing m photons ($m \geqslant 2$) from a linear polarized monochromatic light beam can be expressed as

$$W^{(m)} = 2\pi \left[\frac{2\pi I}{nc\omega^2}\right]^m \sum_{\vec{K}} W_{\vec{K}} \sum_{c,v} |T^{(m)}|^2 \delta(E_c - E_v - m\omega), \tag{5}$$

where n is the refractive index, c the velocity of light in the vacuum, I the incident radiation intensity and $T^{(m)}$ the multiphoton transition amplitude. [Note that the formula (5) corrects two misprints in formula (1) in Ref. 5.] For a given polarization direction $\vec{e}$, $T^{(m)}$ can be written as

TABLE III. Comparison between calculated MPA coefficients $\alpha^{(m)}$ and available experimental data at a given wavelength λ. The unit for $\alpha^{(m)}$ is cm^{2m-3}/GW^{m-1}. Experimental data from Ref. 1 except given otherwise in footnotes.

MX	λ (μm)	Photon number m	Experiments $\alpha^{(m)}$	Present work $\alpha^{(m)}$ in [100]	Zhang *et al.* [d] $\alpha^{(m)}$
NaCl	0.266	2	3.5	2.47	1.2×10^{-1}
	0.397	3	6.9×10^{-4}	1.02×10^{-5}	5.3×10^{-7}
	0.532	4	$(3.45–69)\times10^{-9}$ [a]	1.63×10^{-9}	7.2×10^{-12}
NaBr	0.266	2	2.5	2.81	
KCl	0.266	2	1.7–2.7	1.31	
KBr	0.266	2	1.45–2.0	3.83	1.5
	0.532	4	4.94×10^{-7} [b]	4.99×10^{-8}	2.7×10^{-10}
KI	0.266	2	3.75	2.87	
	0.355	2	7.29	5.05	
	0.532	3	2.9×10^{-3} [c]	1.80×10^{-4}	
	0.694	3	1.77×10^{-3}	1.71×10^{-4}	

[a]From Ref. 24.
[b]From Ref. 25.
[c]From Ref. 26.
[d]From Ref. 5.

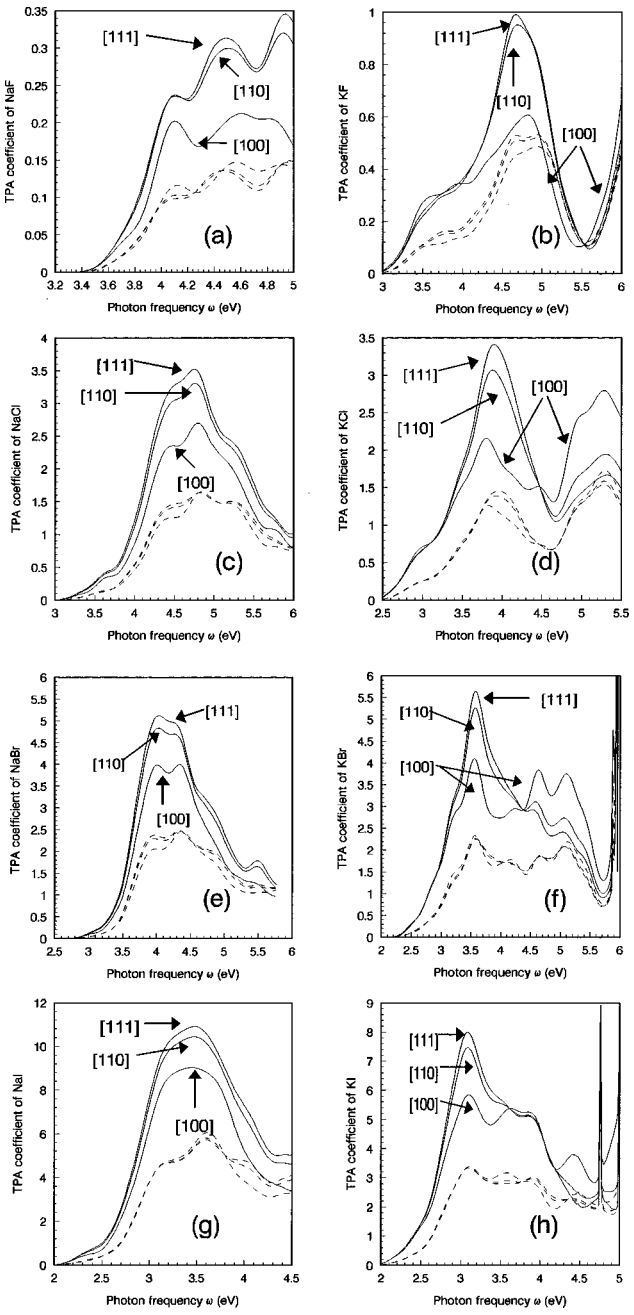

FIG. 3. Polarization dependence of the two-photon absorption (TPA) coefficient of MX (M=Na,K;X=F, Cl, Br, I) in units of cm/GW. The solid lines are for coherent absorption and the dashed lines are for incoherent absorption. Polarized directions are labeled only for coherent absorption.

$$T^{(m)}=\langle c|MG(m-1)MG(m-2)\cdots MG(1)M|v\rangle, \quad (6)$$

where $M=\vec{e}\cdot\vec{p}$ and $G(l)=\Sigma_j|j\rangle\langle j|/(E_j-E_v-l\omega)$, with the summation over j covering all the intermediate states. The m-photon absorption coefficient $\alpha^{(m)}$, related to the m-photon transition probability rate $W^{(m)}$, is

$$\alpha^{(m)}=2m\omega W^{(m)}/I^m. \quad (7)$$

Historically, the analytical calculations of the MPA coefficients usually involved the approximation of the oscillator strengths as well as the energy band and the choice of the intermediate states. They were restricted to a narrow region of nonlinear absorption spectrum, did not consider the coherence effects, and rarely discussed the polarized dependence. The results of simple analytical models were believed to be generally inaccurate and unreliable.[1] The present numerical results are based on the first-principles calculation and thus have a more accurate root than before.

However, to avoid the LAPW failure at the high-lying CB states, we are restricted to the lower-energy photon. To argue the reliability, we rewrite the multiphoton transition amplitude $T^{(m)}$ in a more explicit form, for example, for the two-photon absorption

$$T^{(2)}=\sum_j \frac{\langle c|\hat{\varepsilon}\cdot\vec{p}|j\rangle\langle j|\hat{\varepsilon}\cdot\vec{p}|v\rangle}{E_j-E_v-\omega}. \quad (8)$$

From this expression, the higher the photon energy, the higher the intermediate states are required to be. In practice, only the two-photon absorption in the photon-energy region of $(\frac{1}{2}E_g, E_g)$ is required. In this case, the contribution by high-lying CB's of E_c is attenuated, and as intermediate states, the completeness of low-lying CB's plays a key role in the MPA calculation. As discussed in previous sections, the present band structure is rather good in the low-lying CB's. So we expect the MPA calculation based on the same band wave functions to be meaningful.

B. Numerical results and comparisons

To simplify the calculation, the measured refractive index[11] of MX is adopted in Eq. (5). The truncation energy for intermediate states is set equal to 60 eV. The effect of the Gaussian factor Γ in Eq. (2) on the calculated MPA coefficients is exemplified in Table II for NaCl at certain photon energies. It shows that from $\Gamma=0.10$ to 0.50 eV, the values of two- and three-photon absorption coefficients are stable. For the four-photon absorption coefficient, the choice of Γ changes the MPA value a few times. This large effect only occurs when the photon energy approaches a peak position on the MPA spectrum, e.g., for NaCl in the neighborhood of 532 nm there is a resonant four-photon absorption in the calculation. However, for the estimation of MPA coefficients in a wide energy region, the choice of Γ does not affect the numerical picture seriously.

We compare in Table III the calculated MPA coefficients of MX with the available experimental data. Only the most recently measured ones are listed there. When the original MPA coefficients are given in the generalized m-photon absorption cross section $\sigma^{(m)}$, we use the relation

$$\alpha^{(m)}=2mN\sigma^{(m)}/(\hbar\omega)^{m-1} \quad (9)$$

to translate, where N is the inverse of the volume of the unit cell, assuming that the measurements were conducted on ideal samples.

The calculations are in satisfactory agreement with experiments. The calculated two-photon absorption coefficients are in such good agreement with the measured values for different crystals and different photon energies that their deviation is in fact within the range of the experimental values. The three- and four-photon absorption coefficients are also of the same order of magnitude as the measured ones. The

experimental values are mostly larger than the theoretical ones. The reason may be partly that the present calculation considers only the intrinsic contribution of electronic transitions, while the measured calculations may contain contributions of other processes.

In our previous paper[5] MPA coefficients from the LDA band structure were calculated with the scissors correction, which generally deviates farther from experimental data than the present results (listed in the last column of Table III). In particular, the three- and four-photon absorption coefficients of previous calculations deviate in their order of magnitude from present calculation and experimental results. This shows, as in Sec. III B for linear coefficients, that the scissors correction is generally a bad avenue to optical excitation.

From formula (5) the MPA coefficient is generally dependent on the polarized direction. In fact, the polarization dependence of MPA phenomena is useful in obtaining information about the symmetry of wave function and the positions of higher CB's and deeper VB's. Experimentally, this represents a rather promising proposition. For this reason, we provide in Fig. 3 the two-photon absorption spectra polarized along the [100], [110], and [111] directions. While the three- and four-photon absorption spectra of MX are also calculated,[17] we do not report the results here to save space. We also noted that in traditional analytic approach, Braunstein[23] used a summation of squares of the momentum matrix elements to replace the square of the sum of the matrix elements in formula (5). This is equivalent to considering only the incoherent absorption. We also calculate the incoherent two-photon absorption coefficients in Braunstein's assumption to reveal the nature of the two-photon absorption processes. We summarize some interesting characteristics in two-photon absorption coefficients of MX (Fig. 3) for future comparison with experiments. (i) In general, the coherent absorption is less isotropic and larger than the incoherent absorption. (ii) The two-photon absorption coefficient increases with the atomic number of anions. This trend also holds for higher-order MPA coefficients of MX. (iii) For sodium halides, the two-photon absorption coefficient polarized along the [111] direction has the maximum value and along [100] the minimum value in the whole range from $\frac{1}{2}E_g$ to E_g. For potassium halides, the same relation exists at lower photon energy (see the crossing point in Fig. 3), but changes at the higher photon energy. It appears that in this energy region the K cation orbitals start to influence the optical transition. In a two-photon absorption measurement Liu *et al.*[24] reported no obvious polarization dependence between [110] and [100] of NaCl at 266 nm. From Fig. 3 the estimated difference of NaCl along these two polarized directions in the neighbor of 266 nm is 27%, about the same as the measurement error (about 25–30 %) of Liu *et al.* Thus the dependence of the polarized direction may require more precise experimental setups. (iv) It is worth pointing out that the position of the resonant peaks of the MPA coefficients is always isotropic (this characteristic is shown in the two-photon absorption spectrum of KBr and KI in Fig. 3).

V. CONCLUSION

In procedure outlined above, within the LDA framework, the results of both the linear properties and the MPA coefficients are in satisfactory agreement with the recent experiment. The calculated ε_0 reproduces the systematic trend of MX with respect to the components. The integrated optical oscillator strength of p VB's reveals the mechanism of the optical properties of MX in the low-photon-energy region. The linear optical spectrum in the higher-energy region requires a better description of high-lying CB's and consideration of the contribution of the core excitation and s VB transition. Our calculation shows that the scissors approximation is invalid for ionic crystals for both linear optical and multiphoton properties, although it has been shown to have limited success in semiconductors.

The calculated two-photon absorption coefficients are in good agreement with the experiment. The calculated polarization dependence of two-photon absorption coefficients and their change with respect to the anion elements promote further measurements. The calculated three- and four-photon absorption coefficients are of the same order of magnitudes as but generally smaller than the experiment data. At present we cannot see clearly whether this arises from the limits of the LDA for band energies or the shortcoming of the present LAPW method for the high-lying CB's. Also, it cannot be excluded that this is due to the possible error in the measurement of higher-order MPA. In fact, our calculation is in better agreement with the data from the more recent measurement method[25–27] than the previous ones.[28]

ACKNOWLEDGMENTS

This work was supported by the National Science Foundation of China (Grant No. 19474063). Use of the computing facility from the Computer Network Information Center, Chinese Academy of Sciences and from the National Center of Intelligent Computer is acknowledged.

[1] V. Nathan, A. H. Guenther, and S. S. Mitra, J. Opt. Soc. Am. B **2**, 294 (1985), and references therein.

[2] P. Hohenberg and W. Kohn, Phys. Rev. **136**, B864 (1964); W. Kohn and L. J. Sham, *ibid.* **140**, A1133 (1965).

[3] M. Huang and W. Y. Ching, Phys. Rev. B **47**, 9449 (1993); **47**, 9464 (1993); W. Y. Ching and M. Huang, *ibid.* **47**, 9479 (1993).

[4] W. Y. Ching, F. Gan, and M. Huang, Phys. Rev. B **52**, 1596 (1995).

[5] W. Zhang, Y. Zhou, L. Zhong, X. Nie, and D. Wang, Opt. Commun. **126**, 61 (1996).

[6] R. Adair, L. L. Chase, and S. A. Payne, Phys. Rev. B **39**, 3337 (1989).

[7] Chuangtian Chen, Laser Focus World **XX**, 129 (1989).

[8] S. C. Jones, P. Braunlich, R. T. Casper, X. Shen, and P. Kelly, Opt. Eng. (Bellingham) **28**, 1039 (1989).

[9] H. Krakauer, M. Posternak, and A. J. Freeman, Phys. Rev. B **19**, 1706 (1979).

[10] D. D. Koelling and B. N. Harmon, J. Phys. C **10**, 3107 (1977).

[11] W. J. Tropf, M. E. Thomas, and T. J. Harris, in *Handbook of Optics*, 2nd ed., edited by M. Bass (McGraw-Hill, New York,

1995), Vol. 2, Chap. 33.
[12] See, for example, A. B. Kunz, Phys. Rev. B **26**, 2056 (1982).
[13] F. C. Brown, C. Gähwiller, H. Fujita, A. B. Kunz, W. Scheifley, and N. Carrera, Phys. Rev. B **2**, 2126 (1970).
[14] *Handbook of Optical Constants of Solids*, edited by E. D. Palik (Academic, New York, 1985), pp. 703 and 775.
[15] See, for example, D. Y. Smith, in *Handbook of Optical Constants of Solids* (Ref. 14), Chap. 3.
[16] H. A. Bethe and E. E. Salpeter, *Quantum Mechanics of One- and Two-electron Atoms* (Springer-Verlag, Berlin, 1957), Secs. 61 and 62.
[17] Jun Li, Ph.D dissertation, Institute of Physics, Academia Sinica, 1997.
[18] M. E. Lines, Phys. Rev. B **41**, 3383 (1990).
[19] D. W. Lynch, in *Handbook of Optical Constants of Solids* (Ref. 15), Chap. 10.
[20] D. D. Koelling and G. O. Arbman, J. Phys. F **5**, 2041 (1975).
[21] C. S. Wang and B. M. Klein, Phys. Rev. B **24**, 3417 (1981).
[22] M. S. Hybertsen and S. G. Louie, Phys. Rev. B **34**, 5390 (1986).
[23] R. Braunstein, Phys. Rev. **125**, 475 (1962).
[24] P. Liu, W. L. Smith, H. Lotem, J. H. Bechtel, N. Bloembergen, and R. S. Adhav, Phys. Rev. B **17**, 4620 (1978).
[25] S. C. Jones, A. H. Fischer, P. Braunlich, and P. Kelly, Phys. Rev. B **37**, 755 (1988).
[26] X. A. Shen, S. C. Jones, P. Braunlich, and P. Kelly, Phys. Rev. B **36**, 2831 (1987).
[27] G. Brost, P. Braunlich, and P. Kelly, Phys. Rev. B **30**, 4675 (1984).
[28] I. M. Catalano, A. Cingolani, and A. Minafra, Phys. Rev. B **5**, 1629 (1972); Opt. Commun. **5**, 212 (1972).